

# Impact of Top SiO<sub>2</sub> interlayer Thickness on Memory Window of Si Channel FeFET with TiN/SiO<sub>2</sub>/Hf<sub>0.5</sub>Zr<sub>0.5</sub>O<sub>2</sub>/SiO<sub>x</sub>/Si (MIFIS) Gate Structure

Tao Hu, Xianzhou Shao, Mingkai Bai, Xinpei Jia, Saifei Dai, Xiaoqing Sun, Runhao Han, Jia Yang, Xiaoyu Ke, Fengbin Tian, Shuai Yang, Junshuai Chai, Hao Xu, Xiaolei Wang, Wenwu Wang, and Tianchun Ye

**Abstract**—We study the impact of top SiO<sub>2</sub> interlayer thickness on memory window of Si channel FeFET with TiN/SiO<sub>2</sub>/Hf<sub>0.5</sub>Zr<sub>0.5</sub>O<sub>2</sub>/SiO<sub>x</sub>/Si (MIFIS) gate structure. The memory window increases with thicker top SiO<sub>2</sub>. We realize the memory window of 6.3 V for 3.4 nm top SiO<sub>2</sub>. Moreover, we find that the endurance characteristic degrades with increasing the initial memory window.

**Index Terms**—FeFET, memory window, MIFIS gate structure, charge trapping.

## I. INTRODUCTION

Hafnia(HfO<sub>2</sub>) based silicon channel ferroelectric field-effect transistors (HfO<sub>2</sub> Si-FeFETs) have been extensively studied [1-18], as a strong candidate for non-volatile memory, thanks to the discovery of ferroelectricity in doped-HfO<sub>2</sub> [19]. The memory window (MW) of HfO<sub>2</sub> Si-FeFETs is generally required to be larger than 4 V to meet application in multi-bit memory cells. Recently, inserting a dielectric layer (e.g. SiO<sub>2</sub> or Al<sub>2</sub>O<sub>3</sub>) between the metal gate and ferroelectric layer was found to be an effective method to significantly improve the MW [20-25]. However, the impact of the top SiO<sub>2</sub> interlayer thickness on the MW is still unclear and this hinders the device design. Therefore, we report for the first time the dependence of the MW on the top SiO<sub>2</sub> interlayer thickness in this work. The MW increases with thicker SiO<sub>2</sub>. We realize a maximum MW of 6.3 V by inserting a 3.4 nm SiO<sub>2</sub> top interlayer. Furthermore, we study the dependence of the endurance on initial MW. We find that the endurance characteristic degrades with increasing the initial MW. We realize an initial MW of 5.3 V by inserting a 3.4 nm SiO<sub>2</sub> top interlayer with an endurance of 7×10<sup>3</sup> cycles and a retention of 10 years.

This work was supported by the National Natural Science Foundation of China under Grant No. 92264104 and 52350195. (Corresponding author: Xiaolei Wang)

Tao Hu, Xianzhou Shao, Mingkai Bai, Xinpei Jia, Saifei Dai, Xiaoqing Sun, Runhao Han, Jia Yang, Xiaoyu Ke, Fengbin Tian, Shuai Yang, Junshuai Chai, Hao Xu, Xiaolei Wang, Wenwu Wang, and Tianchun Ye are with Institute of microelectronics of the Chinese Academy of Sciences, Beijing 100029, China. The authors are also with University of Chinese Academy of Sciences, Beijing 100049, China (e-mail: wangxiaolei@ime.ac.cn).

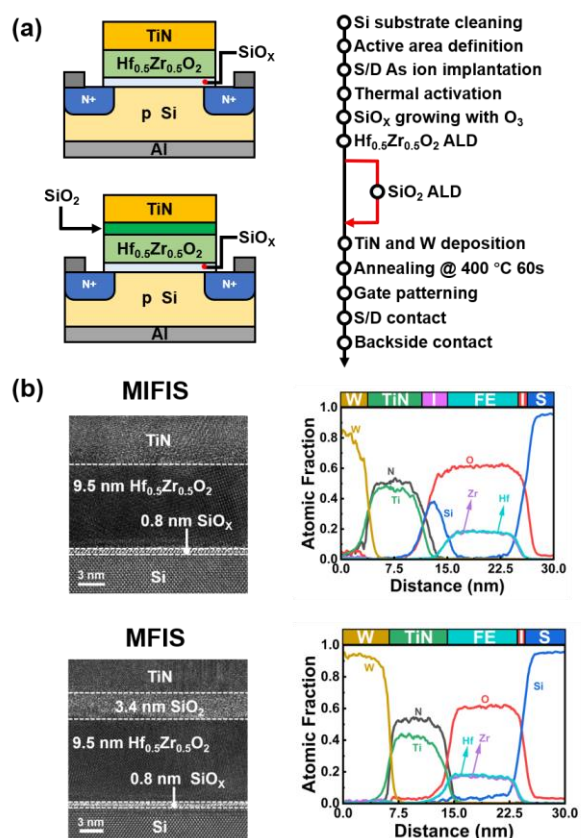


Fig. 1. (a) Schematic of the HfO<sub>2</sub> Si-FeFET device structure and fabrication process flow. (b) HRTEM images and EDS of the MIFIS and MFIS structures.

## II. DEVICE FABRICATION AND CHARACTERIZATION

Fig. 1(a) shows the schematic of the devices and fabrication process flow. In this work, there are two different gate stacks. One is TiN/Hf<sub>0.5</sub>Zr<sub>0.5</sub>O<sub>2</sub>/SiO<sub>x</sub>/Si (MFIS) as the control sample. The other is TiN/SiO<sub>2</sub>/Hf<sub>0.5</sub>Zr<sub>0.5</sub>O<sub>2</sub>/SiO<sub>x</sub>/Si (MIFIS) with a 0.85, 1.7, 2.55, or 3.4 nm SiO<sub>2</sub> top interlayer.

These devices are fabricated in an 8-inch P-type silicon wafer with a resistivity of 8-12 Ω·cm using a gate-last process. Firstly, the source and drain regions are formed by implanting

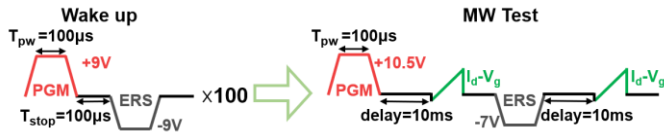


Fig. 2. Details of electrical measurement.

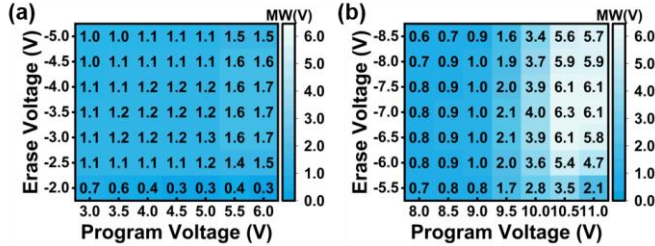


Fig. 3. The MW mapping of (a) MFIS and (b) MIFIS with 3.4 nm SiO<sub>2</sub> as a function of the pulse amplitude under the pulse width of 100  $\mu$ s.

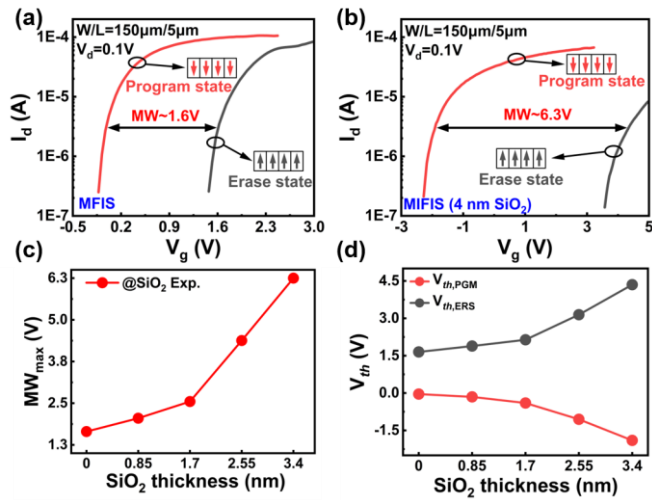


Fig. 4. (a)  $I_d$ - $V_g$  curves of maximum MW for (a) MFIS and (b) MIFIS with 3.4 nm SiO<sub>2</sub> top interlayer. The dependence of the (c) maximum MW and (d)  $V_{th}$  on the top SiO<sub>2</sub> interlayer thickness.

As ions with an energy of 50 KeV and a dose of  $2 \times 10^{15}$  cm<sup>-2</sup>. After that, these devices are annealed at 1050 °C for 5 s under the N<sub>2</sub> atmosphere for dopant activation. Subsequently, the gate stack was formed. The 0.8 nm SiO<sub>x</sub> bottom interlayer was grown by O<sub>3</sub> oxidation at 300 °C. Then, 9.5 nm Hf<sub>0.5</sub>Zr<sub>0.5</sub>O<sub>2</sub> and 0.85-3.4 nm top interlayer SiO<sub>2</sub> were grown by atomic layer deposition (ALD) at 300 °C. After that, 10 nm of TiN and 75 nm W were grown by sputtering. The devices are annealed at 400 °C under an N<sub>2</sub> atmosphere for 60 s to form the orthorhombic phase. Finally, the forming gas annealing (FGA) was performed at 450 °C in 5%-H<sub>2</sub>/95%-N<sub>2</sub>. The gate width/length (L/W) of these devices is 5/150  $\mu$ m. The electrical measures were performed by Keysight B1500A. The threshold voltage ( $V_{th}$ ) is defined by the constant current method.

Fig. 1(b) shows High-Resolution Transmission Electron Microscopy (HRTEM) images and Energy Dispersion Spectrometer (EDS) results for both MIFIS and MFIS structures. For the MIFIS structure, the presence of a peak concentration of Si at the TiN/Hf<sub>0.5</sub>Zr<sub>0.5</sub>O<sub>2</sub> interface confirms the presence of the SiO<sub>2</sub> layer.

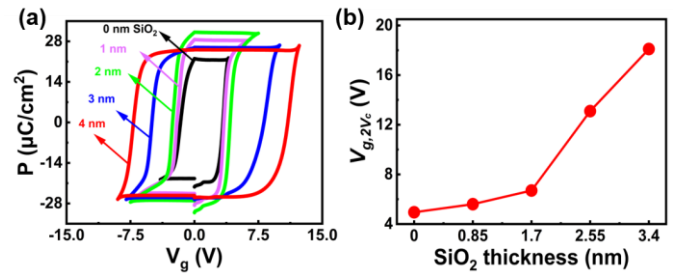


Fig. 5. (a) The results of the PUND measurements. (b) The dependence of  $V_{g,2Vc}$  on the top SiO<sub>2</sub> thickness.

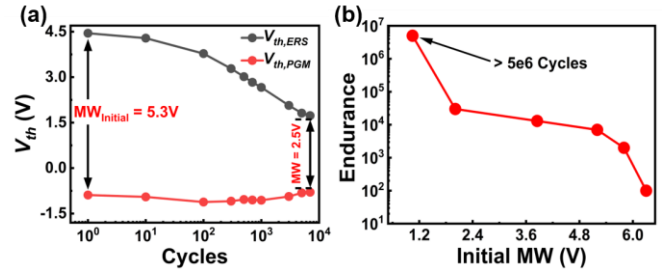


Fig. 6. (a)  $V_{th}$  as a function of cycles for the MIFIS structure with 3.4 nm top SiO<sub>2</sub>. (b) The dependence of endurance on initial MW for MIFIS structure.

### III. RESULTS AND DISCUSSIONS

We investigate the dependence of the MW on pulse Voltage amplitude. Fig. 2 shows the measurement waveforms. The pulse width is set as 100  $\mu$ s. Fig. 3 shows the MW mapping result for the MFIS and MIFIS structure with 3.4 nm SiO<sub>2</sub> (unless specified otherwise in the following context, MIFIS structure refers to the MIFIS structure with the 3.4 nm SiO<sub>2</sub>). The maximum MW is 6.3 V for the MIFIS structure device, while the maximum MW is 1.7 V for the MFIS sample. Fig. 4(a) and (b) show the  $I_d$ - $V_g$  curves corresponding to the maximum MW for the MFIS and MIFIS structures. The physical origin of the larger MW compared with the control sample is due to the charge trapping at the top SiO<sub>2</sub>/Hf<sub>0.5</sub>Zr<sub>0.5</sub>O<sub>2</sub> interface.

We study the impact of top SiO<sub>2</sub> thickness on the maximum MW. Fig. 4(c) shows the impact of top SiO<sub>2</sub> thickness on the maximum MW. The maximum MW increases with thicker top SiO<sub>2</sub> thickness. Fig. 4(d) shows the dependence of the threshold voltage ( $V_{th}$ ) on the top SiO<sub>2</sub> thickness. Fig. 5(a) shows the PUND measurement results. The bulk, source, and drain terminals were shorted during the measurement. The polarization vs gate voltage ( $P$ - $V_g$ ) curve broadens with increasing top SiO<sub>2</sub> thickness. We define the distance between the intersections of the  $P$ - $V_g$  curve and the  $V_g$  axis as  $V_{g,2Vc}$ . Fig. 5(b) shows the dependence of  $V_{g,2Vc}$  on the top SiO<sub>2</sub> thickness.

We conduct the endurance measurement for the MIFIS structure. Fig. 6(a) shows the endurance characteristics of MIFIS structures. The MIFIS sample shows endurance of  $7 \times 10^3$  cycles when the initial MW is 5.3 V. Fig. 6(b) shows the dependence of endurance on the initial MW. The endurance degrades with a larger initial MW.

We study the retention characteristics. Fig. 7 shows the retention characteristics for the two structures. We apply a preset waveform to put the device into the same state before

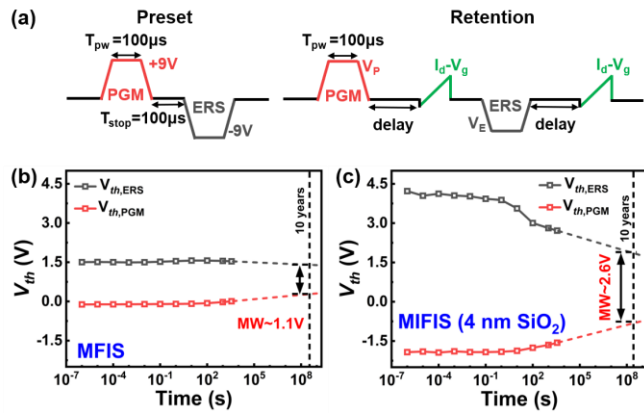


Fig. 7. (a) The measurement waveform of retention. Retention characteristics measured at room temperature of (b) the MFIS structure and (c) the MIFIS structure with 3.4 nm top SiO<sub>2</sub>.

TABLE I  
Comparison of recent research with our work

	Structure	Top IL	MW	Endurance	Retention
Lee et al. from SK Hynix [21] (2022)	MIFIS	SiO <sub>2</sub>	3.8 V	unkonw	10 years
Das et al. from GIT [24] (2023)	MFIFIS	Al <sub>2</sub> O <sub>3</sub>	7.1 V	unknown	10 years
Suzuki et al. from Kioxia [23] (2023)	MIFIS	unkonw	2.3 V	~10 <sup>6</sup> cycles	10 years
Lim et al. from Samsung [22] (2023)	MIFIS	unkonw	3.1 V	~10 <sup>6</sup> cycles	10 years
Yoon et al. from SK Hynix [20] (2023)	MIFIS	unkonw	5.04 V	~3×10 <sup>3</sup> cycles	10 years
Hu et al. from Imecas [25] (2024)	MIFIS	Al <sub>2</sub> O <sub>3</sub>	4.1 V	~1×10 <sup>4</sup> cycles	10 years
This work	MIFIS	SiO <sub>2</sub>	5.8 V	~3×10 <sup>3</sup> cycles	10 years

each retention measurement. Both devices have a retention lifetime beyond 10 years.

Table I shows the benchmark of our work. Our work shows a larger MW (5.8 V) when the endurance is ~3000 cycles and the retention can achieve 10 years.

#### IV. CONCLUSIONS

In this work, we study the impact of the top SiO<sub>2</sub> thickness on the MW. We find that the MW increases with thicker top SiO<sub>2</sub> interlayer. Furthermore, we also investigate the dependence of the endurance on initial MW, and find that the endurance characteristic degrades with increasing the initial MW. By inserting a 3.4 nm top SiO<sub>2</sub> interlayer between the gate metal TiN and the ferroelectric Hf<sub>0.5</sub>Zr<sub>0.5</sub>O<sub>2</sub>, we achieve the MW of 6.3 V with an endurance of 200 cycles. When the MW is ~5.8 V, the endurance can achieve 3000 cycles and the retention is larger than 10 years.

#### REFERENCES

- [1] J. Müller, T. S. Böschke, D. Bräuhaus, U. Schröder, U. Böttger, J. Sundqvist, P. Kücher, T. Mikolajick, and L. Frey, "Ferroelectric Zr<sub>0.5</sub>Hf<sub>0.5</sub>O<sub>2</sub> thin films for nonvolatile memory applications," *Appl. Phys. Lett.*, vol. 99, no. 11, Sept. 2011, doi: 10.1063/1.3636417.
- [2] J. Müller, T. S. Böschke, S. Müller, E. Yurchuk, P. Polakowski, J. Paul, D. Martin, T. Schenk, K. Khullar, A. Kersch, W. Weinreich, S. Riedel, K. Seidel, A. Kumar, T. M. Arruda, S. V. Kalinin, T. Schlösser, R. Boschke, R. v. Bentum, U. Schröder, and T. Mikolajick, "Ferroelectric hafnium oxide: A CMOS-compatible and highly scalable approach to future ferroelectric memories," in *IEDM Tech. Dig.*, Dec. 2013, pp. 10.8.1-10.8.4, doi: 10.1109/IEDM.2013.6724605.
- [3] M. Trentzsch, S. Flachowsky, R. Richter, J. Paul, B. Reimer, D. Utesch, S. Jansen, H. Mulaosmanovic, S. Müller, S. Slesazek, J. Ocker, M. Noack, J. Müller, P. Polakowski, J. Schreiter, S. Beyer, T. Mikolajick, and B. Rice, "A 28nm HKMG super low power embedded NVM technology based on ferroelectric FETs," in *IEDM Tech. Dig.*, Dec. 2016, pp. 11.5.1-11.5.4, doi: 10.1109/IEDM.2016.7838397.
- [4] N. Gong, and T. P. Ma, "Why Is FE-HfO<sub>2</sub> More Suitable Than PZT or SBT for Scaled Nonvolatile 1-T Memory Cell? A Retention Perspective," *IEEE Electron Device Lett.*, vol. 37, no. 9, pp. 1123-1126, Sept. 2016, doi: 10.1109/LED.2016.2593627.
- [5] Z. Cai, K. Toprasertpong, M. Takenaka, and S. Takagi, "HZO Scaling and Fatigue Recovery in FeFET with Low Voltage Operation: Evidence of Transition from Interface Degradation to Ferroelectric Fatigue," in *Proc. Symp. VLSI Technol.*, Jun. 2023, pp. 1-2, doi: 10.23919/VLSITechnologyandCir57934.2023.10185295.
- [6] Y. Peng, W. Xiao, F. Liu, C. Jin, Y. Cheng, L. Wang, Y. Zhang, X. Yu, Y. Liu, Y. Hao, and G. Han, "HfO<sub>2</sub>-ZrO<sub>2</sub> Superlattice Ferroelectric Field-Effect Transistor With Improved Endurance and Fatigue Recovery Performance," *IEEE Trans. Electron Devices*, vol. 70, no. 7, pp. 3979-3982, Jul. 2023, doi: 10.1109/TED.2023.3279063.
- [7] J. Mueller, S. Slesazek, and T. Mikolajick, "Ferroelectric Field Effect Transistor," *Ferroelectricity in Doped Hafnium Oxide: Materials, Properties and Devices*, pp. 451-471, 2019.
- [8] H. Mulaosmanovic, E. T. Breyer, T. Mikolajick, and S. Slesazek, "Recovery of Cycling Endurance Failure in Ferroelectric FETs by Self-Heating," *IEEE Electron Device Lett.*, vol. 40, no. 2, pp. 216-219, Feb. 2019, doi: 10.1109/LED.2018.2889412.
- [9] K. Ni, P. Sharma, J. Zhang, M. Jerry, J. A. Smith, K. Tapily, R. Clark, S. Mahapatra, and S. Datta, "Critical Role of Interlayer in Hf<sub>0.5</sub>Zr<sub>0.5</sub>O<sub>2</sub> Ferroelectric FET Nonvolatile Memory Performance," *IEEE Trans. Electron Devices*, vol. 65, no. 6, pp. 2461-2469, Jun. 2018, doi: 10.1109/ted.2018.2829122.
- [10] U. Schroeder, M. H. Park, T. Mikolajick, and C. S. Hwang, "The fundamentals and applications of ferroelectric HfO<sub>2</sub>," *Nat. Rev. Mater.*, vol. 7, no. 8, pp. 653-669, 2022/08/01. 2022, doi: 10.1038/s41578-022-00431-2.
- [11] N. Tasneem, M. M. Islam, Z. Wang, H. Chen, J. Hur, D. Triyoso, S. Consiglio, K. Tapily, R. Clark, G. Leusink, S. Yu, W. Chern, and A. Khan, "The Impacts of Ferroelectric and Interfacial Layer Thicknesses on Ferroelectric FET Design," *IEEE Electron Device Lett.*, vol. 42, no. 8, pp. 1156-1159, 2021, doi: 10.1109/LED.2021.3088388.
- [12] N. Tasneem, Z. Wang, Z. Zhao, N. Upadhyay, S. Lombardo, H. Chen, J. Hur, D. Triyoso, S. Consiglio, K. Tapily, R. Clark, G. Leusink, S. Kurinec, S. Datta, S. Yu, K. Ni, M. Passlack, W. Chern, and A. Khan, "Trap Capture and Emission Dynamics in Ferroelectric Field-Effect Transistors and their Impact on Device Operation and Reliability," in *IEDM Tech. Dig.*, Dec. 2021, pp. 6.1.1-6.1.4, doi: 10.1109/IEDM19574.2021.9720615.
- [13] A. J. Tan, M. Pešić, L. Larcher, Y. H. Liao, L. C. Wang, J. H. Bae, C. Hu, and S. Salahuddin, "Hot Electrons as the Dominant Source of Degradation for Sub-5nm HfO<sub>2</sub> FeFETs," in *Proc. Symp. VLSI Technol.*, Jun. 2020, pp. 1-2, doi: 10.1109/VLSITechnology18217.2020.9265067.
- [14] S. W. Kim, W. Shin, M. Kim, K. R. Kwon, J. Yim, J. Kim, C. Han, S. Jeong, E. C. Park, J. W. You, H. Kim, R. Choi, and D. Kwon, "Ferroelectric Field-Effect Transistor Synaptic Device With Hafnium-Silicate Interlayer," *IEEE Electron Device Lett.*, vol. 44, no. 12, pp. 1955-1958, 2023, doi: 10.1109/LED.2023.3324695.
- [15] E. J. Shin, S. W. Shin, S. H. Lee, T. I. Lee, M. J. Kim, H. J. Ahn, J. H. Kim, W. S. Hwang, J. Lee, and B. J. Cho, "Capacitance Boosting by Anti-Ferroelectric Blocking Layer in Charge Trap Flash Memory Device," in *IEDM Tech. Dig.*, Dec. 2020, pp. 6.2.1-6.2.4, doi: 10.1109/IEDM13553.2020.9371984.
- [16] K. T. Chen, H. Y. Chen, C. Y. Liao, G. Y. Siang, C. Lo, M. H. Liao, K. S. Li, S. T. Chang, and M. H. Lee, "Non-Volatile Ferroelectric FETs Using 5-nm

- Hf<sub>0.5</sub>Zr<sub>0.5</sub>O<sub>2</sub> With High Data Retention and Read Endurance for 1T Memory Applications,” *IEEE Electron Device Lett.*, vol. 40, no. 3, pp. 399-402. 2019, doi: 10.1109/LED.2019.2896231.
- [17] J. Chai, H. Xu, J. Xiang, Y. Zhang, L. Zhou, S. Zhao, F. Tian, J. Duan, K. Han, X. Wang, J. Luo, W. Wang, T. Ye, and Y. Guo, “First-principles study of oxygen vacancy defects in orthorhombic Hf<sub>0.5</sub>Zr<sub>0.5</sub>O<sub>2</sub>/SiO<sub>2</sub>/Si gate stack,” *J. Appl. Phys.*, vol. 132, no. 10. 2022, doi: 10.1063/5.0106750.
- [18] Q. H. Shao, G. X. Liu, D. Teweldebrhan, A. A. Balandin, S. Runyantsev, M. S. Shur, and D. Yan, “Flicker Noise in Bilayer Graphene Transistors,” *IEEE Electron Device Lett.*, vol. 30, no. 3, pp. 288-290, MAR. 2009, doi: 10.1109/LED.2008.2011929.
- [19] T. S. Bösccke, J. Müller, D. Bräuhäus, U. Schröder, and U. Böttger, “Ferroelectricity in hafnium oxide thin films,” *Appl. Phys. Lett.*, vol. 99, no. 10, Sept. 2011, doi: 10.1063/1.3634052.
- [20] S. Yoon, S. I. Hong, D. Kim, G. Choi, Y. M. Kim, K. Min, S. Kim, M. H. Na, and S. Cha, “QLC Programmable 3D Ferroelectric NAND Flash Memory by Memory Window Expansion using Cell Stack Engineering,” in *Proc. Symp. VLSI Technol.*, Jun. 2023, pp. 1-2, doi: 10.23919/VLSITechnologyandCir57934.2023.10185294.
- [21] J.-G. Lee, J. Kim, D. I. Suh, I. Kim, G. D. Han, S. W. Ryu, S. Lee, M.-H. Na, S. Y. Cha, H. W. Park, and C. S. Hwang, “Memory Window Expansion for Ferroelectric FET based Multilevel NVM: Hybrid Solution with Combination of Polarization and Injected Charges,” in *Proc. IEEE Int. Memory Workshop (IMW)*, May, 2022, pp. 1-4, doi: 10.1109/imw52921.2022.9779292.
- [22] S. Lim, T. Kim, I. Myeong, S. Park, S. Noh, S. M. Lee, J. Woo, H. Ko, Y. Noh, M. Choi, K. Lee, S. Han, J. Baek, K. Kim, J. Kim, D. Jung, K. Kim, S. Yoo, H. J. Lee, S. G. Nam, J. S. Kim, J. Park, C. Kim, S. Kim, H. Kim, J. Heo, K. Park, S. Jeon, W. Kim, D. Ha, Y. G. Shin, and J. Song, “Comprehensive Design Guidelines of Gate Stack for QLC and Highly Reliable Ferroelectric VNAND,” in *IEDM Tech. Dig.*, Dec. 2023, pp. 1-4, doi: 10.1109/IEDM45741.2023.10413820.
- [23] K. Suzuki, K. Sakuma, Y. Yoshimura, R. Ichihara, K. Matsuo, D. Hagishima, M. Fujiwara, and M. Saitoh, “High-Endurance FeFET with Metal-Doped Interfacial Layer for Controlled Charge Trapping and Stabilized Polarization,” in *IEDM Tech. Dig.*, Dec. 2023, pp. 1-4, doi: 10.1109/IEDM45741.2023.10413699.
- [24] D. Das, H. Park, Z. Wang, C. Zhang, P. V. Ravindran, C. Park, N. Afroze, P. K. Hsu, M. Tian, H. Chen, W. Chern, S. Lim, K. Kim, K. Kim, W. Kim, D. Ha, S. Yu, S. Datta, and A. Khan, “Experimental demonstration and modeling of a ferroelectric gate stack with a tunnel dielectric insert for NAND applications,” in *IEDM Tech. Dig.*, Dec. 2023, pp. 1-4, doi: 10.1109/IEDM45741.2023.10413697.
- [25] T. Hu, X. Sun, M. Bai, X. Jia, S. Dai, T. Li, R. Han, Y. Ding, H. Fan, Y. Zhao, J. Chai, H. Xu, M. Si, X. Wang, and W. Wang, “Enlargement of Memory Window of Si Channel FeFET by Inserting Al<sub>2</sub>O<sub>3</sub> Interlayer on Ferroelectric Hf<sub>0.5</sub>Zr<sub>0.5</sub>O<sub>2</sub>,” *IEEE Electron Device Lett.*, pp. 1-1. 2024, doi: 10.1109/LED.2024.3381966.